Retinal Origin of Electrically Evoked Potentials in Response to Transcorneal Alternating Current Stimulation in the Rat

Andrzej T. Foik,[1] Ewa Kublik,[1] Elena G. Sergeeva,[2] Turgut Tatlisumak,[3] Paolo M. Rossini,[4] Bernhard A. Sabel,[2] and Wioletta J. Waleszczyk[1]

[1]Nencki Institute of Experimental Biology, Warsaw, Poland
[2]Institute of Medical Psychology, Medical Faculty, Otto-von-Guericke Universität, Magdeburg, Germany
[3]Department of Neurology, Helsinki University Central Hospital (HUCH), Helsinki, Finland
[4]Institute of Neurology, Department of Geriatrics, Neurosciences & Orthopaedics, Catholic University of Rome and IRCCS S.Raffaele Pisana, Roma, Italy

PURPOSE. Little is known about the physiological mechanisms underlying the reported therapeutic effects of transorbital alternating current stimulation (ACS) in vision restoration, or the origin of the recorded electrically evoked potentials (EEPs) during such stimulation. We examined the issue of EEP origin and electrode configuration for transorbital ACS and characterized the physiological responses to CS in different structures of the visual system.

METHODS. We recorded visually evoked potentials (VEPs) and EEPs from the rat retina, visual thalamus, tectum, and visual cortex. The VEPs were evoked by light flashes and EEPs were evoked by electric stimuli delivered by two electrodes placed either together on the same eye or on the eyeball and in the neck. Electrically evoked potentials and VEPs were recorded before and after bilateral intraorbital injections of tetrodotoxin that blocked retinal ganglion cell activity.

RESULTS. Tetrodotoxin abolished VEPs at all levels in the visual pathway, confirming successful blockage of ganglion cell activity. Tetrodotoxin also abolished EEPs and this effect was independent of the stimulating electrode configurations.

CONCLUSIONS. Transorbital electrically evoked responses in the visual pathway, irrespective of reference electrode placement, are initiated by activation of the retina and not by passive conductance and direct activation of neurons in other visual structures. Thus, placement of stimulating electrodes exclusively around the eyeball may be sufficient to achieve therapeutic effects.

Keywords: visual rehabilitation, transorbital alternating current stimulation, visual pathway, retinal ganglion cells, EEPs, VEPs, visual dysfunctions, electrophysiology

Noninvasive electric current stimulation is a rapidly developing tool to modulate brain excitability for both research and therapeutic approaches to brain dysfunctions.[1–3] Positive therapeutic effects have been observed for various conditions, including poststroke recovery,[4–7] control of epilepsy,[8] tumor therapy,[9] and neuropsychiatric disorders.[10] It is clear that the effects of noninvasive current stimulation greatly depend on therapeutic regimens[1] and the status of the patient at the time of treatment, for example, brain state or recovery stage.[11–14] Thus, the details of the stimulation paradigm, such as electrode placement, stimulus polarity, frequency and pattern of stimulation, as well as the optimal time and duration of stimulation, require further refinement to maximize the therapeutic effects.[15]

Noninvasive current stimulation is also an effective tool in the rehabilitation of visual impairments such as amblyopia,[16,17] hemianopia,[18] glaucoma, and other optic nerve neuropathies.[19–21] However, therapeutic stimulation protocols would significantly benefit from a better understanding of the

functional mechanism(s) of such therapies, which would in turn speed up further refinement of more effective stimulation procedures. For example, it is unclear whether the transorbital alternating current stimulation (ACS) used for the rehabilitation of ophthalmic patients selectively stimulates retinal ganglion cells (RGCs) to generate action potentials and enforces a wave of excitation through the visual pathway to the cortex. Conversely, the ACS could directly and nonspecifically activate brain structures within its electric field. How does the placement of the stimulating electrodes influence such specific and/or nonspecific effects?

There are additional issues that have practical and clinical implications. For example, electrodes used for transorbital ACS of patients with optic nerve damage or glaucoma are located near the eyeball with the reference electrode placed on the arm.[19–21] Such an electrode arrangement could potentially create problems for patients with cardiac dysrhythmia by interfering with cardiac pacemaker function. Pacemaker dysfunction resulting from therapeutic electrical stimulation

has been reported in a case of transcutaneous nerve stimulation.[22] Establishing an alternative and effective electrode placement is, therefore, crucial for the future use of transorbital ACS as a therapeutic tool in standard clinical care, so that patients with pacemakers would not have to be excluded from this new treatment option.

To this end, we compared the responses for different stimulating electrode arrangements before and after blocking RGC activity. Visually and electrically evoked potentials (VEPs and EEPs, respectively) were simultaneously recorded from four structures along the rat's visual pathway: the retina, visual dorsal thalamus, superior colliculus (SC), and the visual cortex (VCx). Electrically evoked potentials were obtained in response to electrical pulse stimulation delivered by using two different electrode arrangements, that is, electrodes were placed on one eyeball (eye–eye arrangement) or on the eyeball and in the neck (eye–neck arrangement). Tetrodotoxin (TTX) was injected into the eyes to block RGC activity as a way of revealing the origin of the EEP. Electrically evoked potentials were abolished after TTX injection regardless of the arrangement of stimulating and reference electrodes. These results demonstrated the retinal origin of the EEPs and suggest that the placement of stimulating electrodes exclusively around the eyeball may be sufficient to achieve therapeutic results.

MATERIALS AND METHODS

Subjects

All experimental procedures were conducted in accordance with the 86/609/EEC Directive and were accepted by the First Warsaw Local Ethical Commission for Animal Experimentation. All efforts were undertaken to limit the number of animals used for the study and avoid their stress and suffering. All procedures adhered to the ARVO Statement for the Use of Animals in Ophthalmic and Vision Research. Animals were cared for in accordance with the Animal Welfare Act and the "Guide for the Care and Use of Laboratory Animals."

The experiments were conducted on 12 adult (250–500 g) male and female Wistar rats obtained from the Medical University of Białystok, Poland. Rats were housed in the Animal House of the Nencki Institute with food and water available ad libitum and maintained on a 12-hour light/dark cycle (light on 7:00 AM). Electrophysiological experiments were performed between 9:00 AM and 7:00 PM.

Surgical Procedures

Rats were anaesthetized with urethane (1.5 g/kg, 30% aqueous solution, intraperitoneally; Sigma-Aldrich, Munich, Germany) and placed in a stereotaxic apparatus. The depth of anesthesia was controlled by checking for the presence of a withdrawal reflex and by monitoring the electrocorticogram (ECoG). Additional doses of urethane (0.15 g/kg) were administered when high-frequency, low-amplitude activity dominated the ECoG. Body temperature was maintained at 37°C–38°C by using an automatically controlled electric heating blanket, and fluid requirements were fulfilled by subcutaneous injections of 0.9% NaCl (2 mL every 2–3 hours). The skin on the head was swabbed with iodine and then a local anesthetic (lidocaine hydrochloride, Lidocaine 0.5%, 1 mL; Polfa Warszawa S.A., Warsaw, Poland) was injected subcutaneously along the incision line. The skull was exposed and trephined (1 mm in diameter) in areas overlaying the binocular VCx contra- and ipsilateral to the stimulated eye:

6.0 to 7.5 mm posterior to bregma, 4.0 mm lateral from the midline; contralateral visual thalamus: 4.1 to 4.8 mm posterior to bregma, 4.2 mm lateral; contralateral SC: 7.0 mm posterior to bregma, 1.5 mm lateral (see Fig. 1). Stereotaxic measurements were based on the rat brain atlas of Paxinos and Watson.[23] Both eyes remained open to allow binocular presentation of visual stimuli. Corneas were lubricated with Lacrimal (Polfa Warszawa S.A.) as required to prevent drying.

Local Field Potential, ECoG, and Retinal Light Evoked Potential Recording

Continuous spontaneous neuronal activity, EEP, and VEP recordings were performed in all animals. In six rats, silver/silver chloride (Ag/AgCl) surface ball electrodes were used to record the ECoG from the primary VCx contralateral to the stimulated eye (7–7.5 mm posterior to bregma, 4 mm lateral). Bipolar recordings were achieved by using a reference ball electrode placed over the ipsilateral retrosplenial dysgranular cortex (6–6.5 posterior to bregma; 1 mm lateral). In the other six rats, visual signals were recorded with monopolar, custom-made linear electrodes made of microwire (25-µm tungsten in HML insulation; California Fine Wire, Gover Beach, CA, USA) or with silicon probe electrode arrays (NeuroNexus Technologies, Ann Arbor, MI, USA) with an Ag/AgCl ground-reference wire positioned in the neck muscles. Thalamic and SC recording probes consisted of eight and seven wires, respectively, with a vertical recording site separation of ~200 µm. This vertical arrangement of recording sites increased the chances of successfully recording from the desired structure. Cortical recordings were made by using 16-channel silicon probes with an interelectrode distance of 150 µm. Electrode tips recording from the VCx, dorsal visual thalamus, and SC were lowered to 2.1, 4, and 5.4 mm from the cortical surface, respectively. Light evoked responses from the retina were recorded with a silver wire electrode placed on the cornea close to the edge of the lower lid. The signals were bandpass filtered between 0.3 and 5 kHz and amplified (×500) by using 16-channel differential AC amplifiers (A-M Systems, Sequim, WA, USA). Recorded signals, regardless of electrode type, were digitized (10-kHz sampling rate), fed to a personal computer for online display, analysis, and data storage via a Power 1401 multichannel data acquisition interface and Spike2 software (Cambridge Electronic Design, Cambridge, UK). A custom written program was used for data acquisition and control of the visual and electrical stimulation. Stimulation marks were recorded along with the electrophysiological signals in the same data file.

Stimulation Paradigm

To record VEPs and EEPs during a similar general brain state, we applied visual and electrical stimuli in rotation (Fig. 1C). Time intervals from 2 to 3 seconds between consecutive stimuli consisted of a 2-second constant component plus a variable component that was randomly selected by the program (value between ~4 ms and 1 second). Consequently, the interval between two stimuli of the same type (e.g., two electrical or two visual stimuli) ranged from 4 to 6 seconds.

Visual Evoked Potentials

Visual evoked potentials recorded from the contralateral binocular zones of the VCx, dorsal thalamus, and SC were obtained in response to flashing white-light–emitting diodes (LEDs) placed 10 cm in front of the rat. The stimulus (7600 cd/m^2 luminance, 2-ms duration) was repeated 300 times with an interstimulus interval randomly ranging between 4 to 6
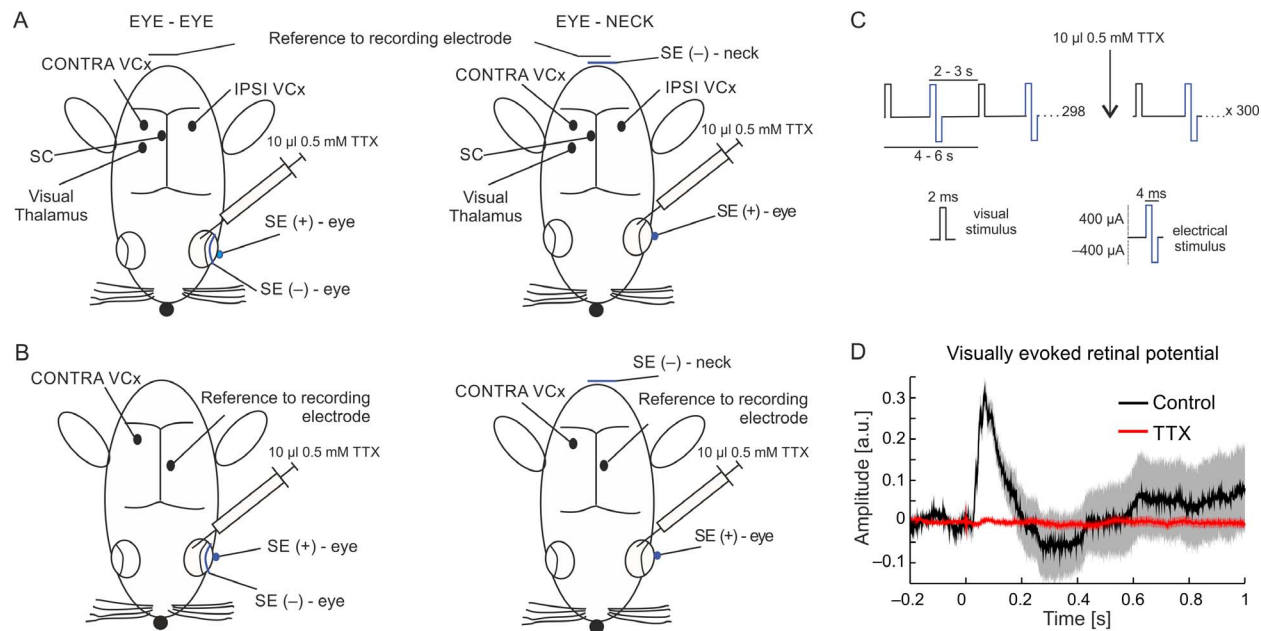
FIGURE 1. (**A, B**) Schematic representation of the dorsal view of the rat head showing the various positions of recording and stimulating electrodes. Stimulating electrodes of positive and negative polarity (SE[+] and SE[−]) were placed either on the eyeball (eye–eye configuration, *left panels* in [**A**] and [**B**]) or one on the eyeball and the other in the neck (eye–neck configuration, *right panels* in [**A**] and [**B**]). (**A**) Schematic diagram showing the points of insertion of linear vertical electrode arrays aimed at subcortical structures contralateral to the stimulated eye (visual thalamus–dorsal lateral geniculate nucleus, lateral posterior nucleus; SC; contra- and ipsilateral visual cortex [contra VCx, ipsi VCx]). The reference electrode was placed in neck muscles and grounded. (**B**) Schematic diagram showing surface electrode placement for recording from the contralateral VCx with the reference electrode located on the ipsilateral retrosplenial dysgranular cortex (differential recording, reference not grounded). (**C**) Stimulation paradigm. The *upper graph* demonstrates the timing of consecutive intermingled visual and electric stimuli, 300 of each in the control period and after TTX injection. The 2- to 3-second range corresponds to randomly selected intervals between visual and electrical stimuli (see Methods for details). The 4- to 6-second range corresponds to the interval between two consecutive electrical or two consecutive visual stimuli. The *lower graph* represents the impulses used for evoking light flashes and electric stimuli. (**D**) Averaged ($n = 300$) VEPs obtained before (*black line with grey* $\pm$ SEM corridor) and after bilateral TTX injections (10 µL, 0.5 mM) (*red line with pink* $\pm$ SEM corridor) into the vitreous humor. The recording electrode (silver wire) was placed on the cornea close to the edge of the lower lid.

seconds and was intermingled with transcorneal electrical stimulation (Fig. 1C).

Transcorneal ACS and Electrically Evoked Potentials

Two different stimulating electrode configurations were tested; eye–eye and eye–neck (Figs. 1A, 1B). The eye–eye configuration consisted of two electrodes: an Ag/AgCl wire (0.2-mm thick) ring (5-mm inner diameter) placed on the cornea and an Ag/AgCl ball (1-mm diameter) placed inside the ring (Figs. 1A, 1B, left panels). The eye–neck configuration consisted of a corneal bulb electrode and an Ag/AgCl wire placed in the neck muscles.

Electrically evoked potentials recorded from the regions detailed above were obtained by applying squared biphasic current pulses (2 ms per phase, with 800-µA peak-to-peak amplitudes; Fig. 1C). Pulse parameters that produced a clear EEP were optimized during the first experiment and then used for all experiments. Single pulses were delivered by a MASTER8 stimulator (A.M.P.I., Jerusalem, Israel) and a linear stimulus isolator unit (World Precision Instruments, Sarasota, FL, USA). For each stimulating electrode arrangement, 300 pulses were delivered in 4- to 6-second intervals, intermingled with VEP stimuli (Fig. 1C).

Inactivation of RGCs

After recording the responses for both stimulating configurations, TTX (10 µL, 0.5 mM; TOCRIS, Bristol, UK) was injected bilaterally into the posterior chamber of the eye with a 10 µL

Hamilton syringe. Effectiveness of RGC inactivation was assessed by recording retinal responses to visual stimulation (300 flashes; Fig. 1D) via a silver electrode placed on the cornea close to the edge of the lower lid, and by simultaneously monitoring VEPs in the other visual areas. Following abolition of any light response, a second set of recordings was performed from the same areas and consisted of 300 VEPs intermingled with 300 EEPs starting approximately 10 minutes after TTX injections.

Histology

Standard histologic techniques were used to verify placement of the electrodes (Fig. 2). Electrodes coated with DiI (1,I′-dioctadecyl-3.3,3′,3′ tetramethyl-indocarbocyanine perchlorate; Sigma-Aldrich, Munich, Germany) were used in some cases to facilitate electrode tract reconstruction.[24] Rats were injected with an overdose of Nembutal (150 mg/kg; Abbott Laboratories, North Chicago, IL, USA) at the end of the experiment and perfused through the heart with 4% paraformaldehyde in phosphate buffered saline. The brains were removed, stored in paraformaldehyde and 30% sucrose for cryoprotection, then cut into 50-µm slices, and stained with cresyl violet and/or cytochrome oxidase. Data obtained from incorrect electrode placements were excluded from further analysis.

Data Analysis and Statistics

All off-line data analysis was performed in Matlab R2010B (MatWorks, Natick, MA, USA) using custom written programs.
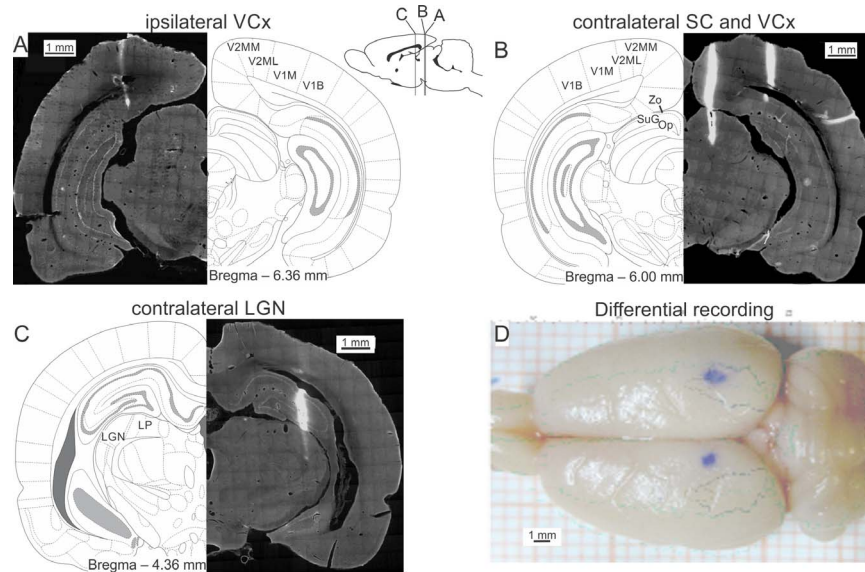
FIGURE 2. Histologic verification of the recording sites. Recording electrodes were labeled with DiI, allowing later track visualization with fluorescent microscopy. (**A**) Ipsilateral VCx. V1M and V1B: monocular and binocular area of primary VCx, respectively. V2MM and V2ML: mediomedial and mediolateral area of secondary VCx, respectively. *Insert* indicates levels of coronal sections shown in (**A–C**). Section drawings were modified from the Paxinos and Watson atlas.[23] Reprinted with permission from Paxinos G, Watson C. *The Rat Brain in Stereotaxic Coordinates*. 6th ed. San Diego, CA: Academic Press, Inc.; 2007. Copyright 2007 Elsevier. The distance between the sections and bregma is shown below each drawing. (**B**) Superior colliculus and contralateral VCx. Superior colliculus layers: zonal (Zo); superficial grey (SuG); optic (Op). (**C**) Lateral geniculate nucleus and LP nucleus. (**D**) *Top view* of the whole rat brain with surface recording electrode locations marked with crystal violet applied over craniotomies at the completion of the experiment (*blue dots*). *Lines* indicate borders of VCx according to 3D brain atlas of Majka et al.[27]

All data sets obtained from each animal were normalized by a commonly used z-score standardization method, that is, the mean signal value of all recordings made for single rat was subtracted from each data point, which was then divided by the signal standard deviation calculated for all recordings from single animal. For further analysis, we extracted single trial sweeps (from 0.2 second before to 1 second after the stimulus), and from each we subtracted its mean prestimulus potential level. Twenty-millisecond windows encompassing the stimulus artefact were then substituted by zeros to avoid the deformation resulting from data filtering. Interference and noise in the data were removed with the Matlab Chronux toolbox,[25] and the signal was filtered with low pass forward and backward filters (120-Hz cutoff frequency, Kaiser window, factor beta = 4) and down-sampled to 1 kHz. Differences between the responses before and after TTX were assessed by comparing the peak-to-peak amplitudes of the evoked potentials. Differences between EEPs and VEPs are given as the ratio of the normalized amplitude values of both EPs (EEP/VEP). Results are given as the mean ± SD. The Wilcoxon test was used to verify any statistically significant differences in the EP amplitudes.[26] Differences were considered significant at $P \leq$ 0.05 for two-tailed tests.

RESULTS

The multielectrode array positions were histologically verified in six rat brains (see Fig. 2) confirming the proper positioning within the primary VCx (both hemispheres, spanning a depth of 2200 µm; Figs. 2A, 2B), the SC (superficial and intermediate layers; Fig. 2B), and the visual thalamus, that is, the dorsal lateral geniculate nucleus (LGN) ($n = 5$; Fig. 2C) and the lateral posterior nucleus (LP; $n = 1$). Recording in the ipsilateral VCx of one rat had to be rejected owing to technical problems.

The location of surface ECoG electrodes in another six rats was confirmed electrophysiologically without further histologic analysis. A typical placement of a surface ECoG electrode is shown in Figure 2D.

Visual Evoked Potentials

We obtained visual responses to LED flash stimuli in all tested structures for both recording electrode configurations. Examples are shown in Figures 3 and 4. Visual evoked potentials recorded from ECoG electrodes at the cortical surface (Fig. 4) were initially positive, while those from the intracortical arrays showed a typical reversal of potential polarity occurring within granular layer 4[28] (not shown here) and were initially negative in the infragranular layers (Figs. 3A, 3B). Visual evoked potentials recorded in the thalamic structures (LGN and LP) were dominated by waves of negative polarity (Figs. 3C, 3D), while those in SC were characterized by a biphasic oscillatory pattern (Fig. 3E).

Electrically Evoked Potentials

Electrical stimuli intermingled with the presentation of light flashes also evoked responses in all tested structures (see Figs. 3 and 4). Both stimulating electrode arrangements proved to be efficient in evoking responses in the visual system. The current stimulation parameters used in our study (squared biphasic pulses, 4-ms duration with 800-µA peak-to-peak amplitude) resulted in EEP wave polarities that were similar to VEP waves recorded during the same session, but on average had lower amplitudes (EEP/VEP ratio < 1, Table 1). The statistical significance of the amplitude differences between EEPs and VEPs recorded at the same locations were tested with a two-tailed Wilcoxon test (for *P* values see Table 1).
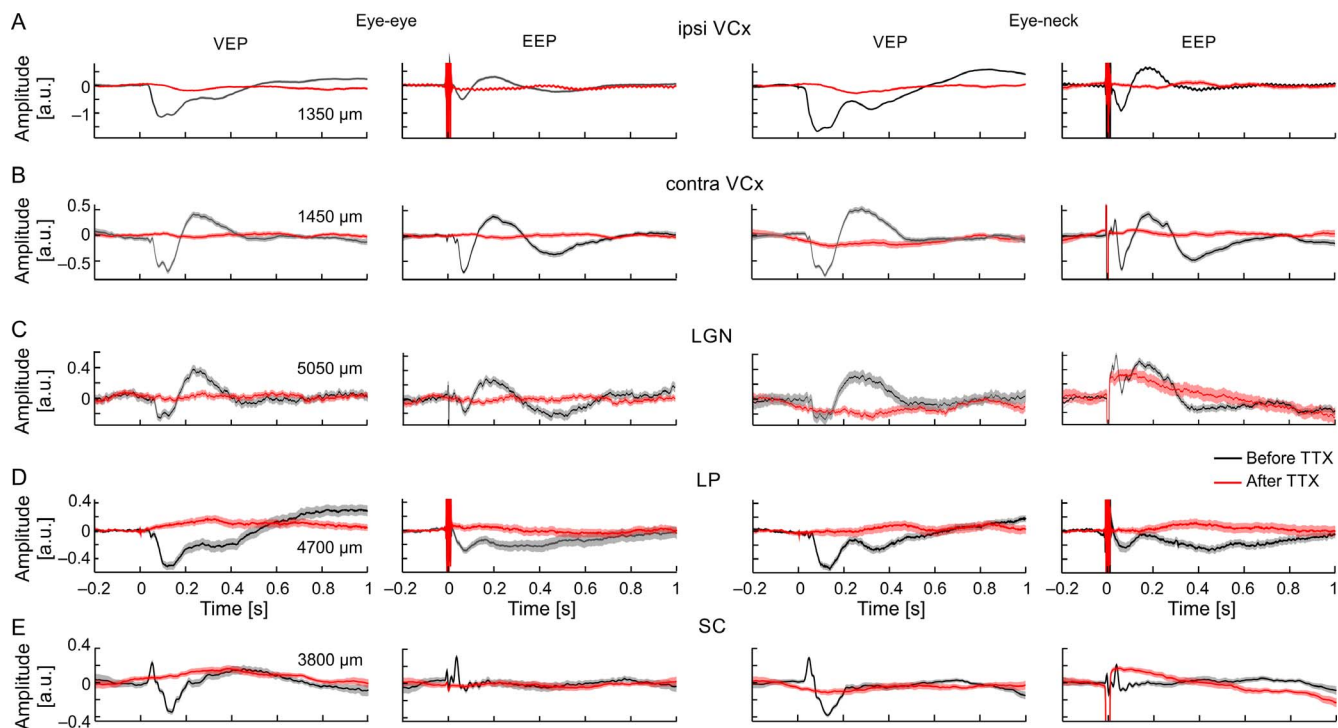
FIGURE 3. Averaged ($n = 300$) visually (VEP) and electrically (EEP) evoked potentials recorded from four structures before (*black lines with grey* ± SEM corridor) and after (*red lines with pink* ± SEM corridors) intraorbital TTX injections. *Tracings* can be compared for eye-eye and eye-neck stimulating electrode configurations. Depths of records (distance from the cortical surface) are indicated in the leftmost column. (**A–E**) Evoked responses recorded from the ipsilateral VCx, contralateral VCx, LGN, LP, and SC. *Plots* show full decay of the responses after TTX injection for both electrode configurations.

Block of Retinal Activity With TTX

We wished to determine if the effects of transorbital ACS were mediated by RGC activity or resulted from direct stimulation of visual structures in the brain. Tetrodotoxin is a well-known sodium channel blocker that prevents action potential generation by RGCs if injected into the vitreous humor.[29] Therefore, we used binocular TTX injections (10 μL) to block visual information leaving the retina. Blockage of RGC spike generation was confirmed by a flattening of the visually evoked retinal response ($n = 6$, $P = 0.03$, two-tailed Wilcoxon test; see Fig. 1D), which was observed shortly after the start of visual stimulation and recording (~2–3 minutes after the TTX injection). Visual evoked potentials and EEPs in other visual structures were abolished coincidently with the blockage of RGC activity for both stimulating electrode configurations in all experimental animals. Mean VEPs and EEPs obtained from the recorded structures in one rat before (black lines) and after TTX injection (red lines in all panels) are shown in Figure 3. A

comparison of EEP amplitudes before and after TTX injection (two-tailed Wilcoxon test) is shown in Table 2. Significant differences between EEP amplitudes before and after TTX injections were observed for all structures except the ipsilateral VCx, where the nonsignificant P value (>0.05) was probably due to the low number of potentials ($n = 5$) used for the comparison.

We observed residual amplitudes after TTX injection (Table 2), and these may correspond to changes in the level of the signal due to saturation of the amplifier following stimulation pulses but do not represent true responses. The amplitudes of the small waves observed post stimulus after the TTX injection were not significantly different from the spontaneous fluctuations in the prestimulus baseline recordings. We cannot, however, entirely exclude the possibility that small residual responses may still be present from activation of TTX-resistant Na$^+$ currents.[30]

We used surface electrodes (ECoG) and differential recordings from two cortical areas to exclude the possibility that the
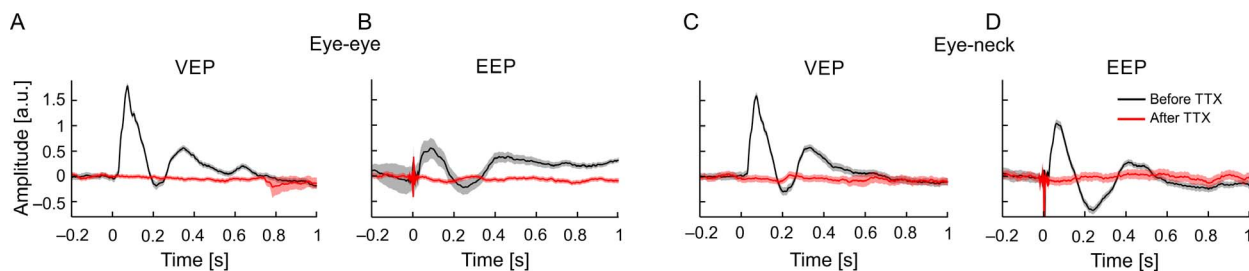
FIGURE 4. Evoked potentials observed in the ECoG recorded as a differential signal between VCx and the retrosplenial dysgranular cortex (reference) before (*black line*) and after (*red line*) TTX injections: eye-eye (**A, B**) and eye-neck configurations (**C, D**). Averaged responses over 300 stimulus repetitions are shown. The corridors around mean traces indicate SEMs. Note the decay in the VEP and EEP responses after TTX injections.

TABLE 1. Summary Data for EEP Versus VEP Amplitude Comparisons for a Two-Electrode Configuration (Eye–Eye and Eye–Neck)*

	Eye–Eye EEP/VEP Ratio ± SD	EEP–VEP Difference, P	Eye–Neck EEP/VEP Ratio ± SD	EEP–VEP Difference, P
Thalamus ($n = 6$)†	0.68 ± 0.26	0.03	0.69 ± 0.25	0.06
SC ($n = 6$)†	0.51 ± 0.18	0.03	0.43 ± 0.22	0.03
Contralateral VCx ($n = 6$)†	0.59 ± 0.34	0.06	0.38 ± 0.09	0.03
Ipsilateral VCx ($n = 5$)†	0.35 ± 0.16	0.06	0.36 ± 0.25	0.06
VCx versus contralateral dysgranular Cx ($n = 6$)‡	0.25 ± 0.15	0.03	0.3 ± 0.15	0.03

* Columns 2 and 4 represent the average values of EEP and VEP amplitude ratios; columns 3 and 5 give P values from two-tailed Wilcoxon test for the difference between EEP and VEP amplitudes.
† Monopolar registration.
‡ Differential registration.

stimulating electrode in the neck muscles in the eye–neck configuration was electrically coupled to the neck reference electrodes, and grounded. Electrically evoked potential and VEP responses were recorded from primary VCx with the reference electrode (not grounded) placed over the retrosplenial dysgranular cortex (Fig. 2D). There was a small difference between epicortical EEPs such that stimulation in the eye–neck configuration evoked responses that were larger versus those obtained for the eye–eye configuration (Table 1). As was the case with monopolar depth recordings, visually and electrically evoked epicortical responses disappeared after TTX injections (Fig. 4A-D, red lines) regardless of the stimulating electrode configuration (Table 2).

DISCUSSION

Noninvasive ACS has recently been shown to be clinically effective in improvement of visual functions in patients.[16-21] Previous reports concerning restoration of vision in glaucoma after transorbital ACS have not determined whether any of the physiological changes observed in patients with vision loss are due exclusively to stimulation of the retina or due to direct stimulation of visual centers in the brain by changes of the field potential. Our results are compatible with the hypothesis of a retinal origin of the EEPs and indicate the importance of early stages of visual information processing on the transorbital ACS. In our acute rat experiments, EEPs and VEPs were recorded from various visually active structures, and after intraocular injections of TTX we observed an immediate and full decay of the EPs, regardless of the electrode configuration. In addition, the data suggest that placing the stimulating electrodes around the eyeball may be sufficient to achieve therapeutic results.

Our conclusion is strengthened by the results reached by Sergeeva and colleagues,[31] indicating that the integrity of the structures at the early stages of visual processing are important for aftereffects obtained with transorbital ACS.

Transorbital ACS: A Mechanistic Hypothesis

Transcranial ACS of the visual system has been shown to elevate the alpha power in EEG recordings obtained from healthy individuals,[12,32,33] and thus possibly has the potential to modify alpha band–dependent visual functions.[34,35] An elevation in alpha power has also been shown to occur after transorbital ACS in patients with visual field loss and appears to be an effective tool to induce some vision restoration after optic nerve injury.[21,36] Ten days of repetitive transorbital ACS given to patients with optic nerve damage results in a reduction of visual deficits expressed as an enlargement of the visual fields, improved visual acuity, faster reaction times, and improved vision-related quality of life.[19-21,37] The postulated therapeutic mechanisms for this improvement are synchronization of activity in the visual pathway and interference with ongoing oscillatory brain activity, in addition to connectivity changes at higher stages of visual processing.[38,39] The complete abolition of EEPs following RGC activity blockage by TTX strongly supports the hypothesis that ACS enforces a wave of excitation flowing through the visual pathway with a retinal origin rather than directly activating neurons in downstream visual structures via passive conductance. This suggests that transorbital ACS renders its effect via synchronization of spike firing in the ascending retinogeniculate and extrageniculate pathways. Indeed, spike synchrony of converging input enhances the transfer of information and speeds up processing.[40,41] Synchronized retinal input to the LGN most likely results in synchronized thalamocortical input, which in turn, maximizes the reliability of cortical responses.[42] Synchronization of the neuronal activity is not the only effect of current stimulation that one can expect. Aftereffects of current stimulation in the visual system include neuronal protection and plasticity through synaptic strength modifications.[43-45] Repetitive ACS stimulation, which effectively activates the VCx over time, may result in an increased efficacy of thalamocortical synaptic function, which is similar to long-

TABLE 2. Summary Data for EEP Amplitudes Before and After TTX Injections for the Two Electrode Configurations

Structure	Eye–Eye Electrode Configuration			Eye–Neck Electrode Configuration		
	EEP (a.u.*) Before TTX	EEP (a.u.*) After TTX	P Value	EEP (a.u.*) Before TTX	EEP (a.u.*) After TTX	P Value
Thalamus ($n = 6$)†	0.36 ± 0.16	0.08 ± 0.04	0.03	0.39 ± 0.2	0.09 ± 0.07	0.03
SC ($n = 6$)†	0.56 ± 0.22	0.05 ± 0.03	0.03	0.55 ± 0.38	0.06 ± 0.04	0.03
Ipsilateral VCx ($n = 5$)†	0.25 ± 0.13	0.04 ± 0.02	0.06	0.34 ± 0.34	0.07 ± 0.02	0.06
Contralateral VCx ($n = 6$)†	0.54 ± 0.26	0.05 ± 0.02	0.03	0.43 ± 0.19	0.07 ± 0.04	0.03
VCx versus dysgranular Cx ($n = 6$)‡	0.3 ± 0.3	0.05 ± 0.04	0.03	0.3 ± 0.16	0.05 ± 0.04	0.03

* Arbitrary units after z-score normalization, mean ± SD.
† Monopolar recording.
‡ Differential recording; P values from two-tailed Wilcoxon test comparing EEP amplitudes before and after TTX.

Investigative Ophthalmology & Visual Science

term potentiation, and finally leads to a stable improvement in the transfer of visual information to the VCx. The effects of ACS observed at higher stages of visual cortical processing thus seem to be secondary to the effects evoked by transorbital ACS at the lower stages of the visual pathway.

Summary and Conclusions

The retinal origin of EEPs, regardless of the location of the reference electrode, suggests that placement of stimulating electrodes around the eyeball may be sufficient to achieve therapeutic effects. Our results indicate the importance of the early stages of visual processing in generating EEPs in transorbital ACS and argue that synchronization of retinal input to the thalamus and tectum is a major mechanism of action in transorbital ACS. However, we cannot completely rule out a direct influence of current stimulation on the ongoing brain activity through other brain structures. Indeed, we observed that epicortical evoked responses differed for eye–neck versus eye–eye configurations. This indicates that various elements of the cortical network can be engaged with different response strengths to the ACS depending on electrode placement. Thus, depending on the electrode placement, ACS may exert different influences on brain function that could render different therapeutic and/or side effects. This issue needs further study.

References

1. Antal A, Paulus W. Transcranial alternating current stimulation (tACS). *Front Hum Neurosci*. 2013;7:317.

2. Utz KS, Dimova V, Oppenländer K, Kerkhoff G. Electrified minds: transcranial direct current stimulation (tDCS) and galvanic vestibular stimulation (GVS) as methods of non-invasive brain stimulation in neuropsychology—a review of current data and future implications. *Neuropsychologia*. 2010; 48:2789–2810.

3. Flöel A. tDCS-enhanced motor and cognitive function in neurological diseases. *Neuroimage*. 2014;85:934–947.

4. Edwardson MA, Lucas TH, Carey JR, Fetz EE. New modalities of brain stimulation for stroke rehabilitation. *Exp Brain Res*. 2013;224:335–358.

5. Grefkes C, Fink GR. Disruption of motor network connectivity post-stroke and its noninvasive neuromodulation. *Curr Opin Neurol*. 2012;25:670–675.

6. Landi D, Rossini PM. Cerebral restorative plasticity from normal ageing to brain diseases: a "never-ending story." *Restor Neurol Neurosci*. 2010;28:349–366.

7. Plow EB, Obretenova SN, Fregni F, Pascual-Leone A, Merabet LB. Comparison of visual field training for hemianopia with active versus sham transcranial direct cortical stimulation. *Neurorehabil Neural Repair*. 2012;26:616–626.

8. Berényi A, Belluscio M, Mao D, Buzsáki G. Closed-loop control of epilepsy by transcranial electrical stimulation. *Science*. 2012;337:735–737.

9. Kirson ED, Dbalý V, Tovarys F, et al. Alternating electric fields arrest cell proliferation in animal tumor models and human brain tumors. *Proc Natl Acad Sci U S A*. 2007;104:10152–10157.

10. Kuo MF, Paulus W, Nitsche MA. Therapeutic effects of non-invasive brain stimulation with direct currents (tDCS) in neuropsychiatric diseases. *Neuroimage*. 2014;85:948–960.

11. Dimyan MA, Cohen LG. Neuroplasticity in the context of motor rehabilitation after stroke. *Nat Rev Neurol*. 2011;7:76–85.

12. Neuling T, Rach S, Herrmann CS. Orchestrating neuronal networks: sustained after-effects of transcranial alternating current stimulation depend upon brain states. *Front Hum Neurosci*. 2013;7:161.

13. Schulz R, Gerloff C, Hummel FC. Non-invasive brain stimulation in neurological diseases. *Neuropharmacology*. 2013;64:579–587.

14. Silvanto J, Muggleton N, Walsh V. State-dependency in brain stimulation studies of perception and cognition. *Trends Cogn Sci*. 2008;12:447–454.

15. Schmidt S, Scholz M, Obermayer K, Brandt SA. Patterned brain stimulation, what a framework with rhythmic and noisy components might tell us about recovery maximization. *Front Hum Neurosci*. 2013;7:325.

16. Spiegel DP, Byblow WD, Hess RF, Thompson B. Anodal transcranial direct current stimulation transiently improves contrast sensitivity and normalizes visual cortex activation in individuals with amblyopia. *Neurorehabil Neural Repair*. 2013;27:760–769.

17. Spiegel DP, Li J, Hess RF, et al. Transcranial direct current stimulation enhances recovery of stereopsis in adults with amblyopia. *Neurotherapeutics*. 2013;10:831–839.

18. Plow EB, Obretenova SN, Halko MA, et al. Combining visual rehabilitative training and noninvasive brain stimulation to enhance visual function in patients with hemianopia: a comparative case study. *PM R*. 2011;9:825–835.

19. Fedorov A, Jobke S, Bersnev V, et al. Restoration of vision after optic nerve lesions with noninvasive transorbital alternating current stimulation: a clinical observational study. *Brain Stimul*. 2011;4:189–201.

20. Gall C, Sgorzaly S, Schmidt S, Brandt S, Fedorov A, Sabel BA. Noninvasive transorbital alternating current stimulation improves subjective visual functioning and vision-related quality of life in optic neuropathy. *Brain Stimul*. 2011;4:175–188.

21. Sabel BA, Fedorov AB, Naue N, Borrmann A, Herrmann C, Gall C. Non-invasive alternating current stimulation improves vision in optic neuropathy. *Restor Neurol Neurosci*. 2011;29:493–505.

22. Chen D, Philip M, Philip PA, Monga TN. Cardiac pacemaker inhibition by transcutaneous electrical nerve stimulation. *Arch Phys Med Rehabil*. 1990;71:27–30.

23. Paxinos G, Watson C. *The Rat Brain in Stereotaxic Coordinates*. 6th ed. San Diego, CA: Academic Press, Inc.; 2007.

24. DiCarlo JJ, Lane JW, Hsiao SS, Johnson KO. Marking microelectrode penetrations with fluorescent dyes. *J Neurosci Methods*. 1996;64:75–81.

25. Bokil H, Andrews P, Kulkarni JE, Mehta S, Mitra PP. Chronux: a platform for analyzing neural signals. *J Neurosci Methods*. 2010;192:146–151.

26. Siegel S. *Nonparametric Statistics: For the Behavioral Sciences*. New York: McGraw-Hill; 1956.

27. Majka P, Kublik E, Furga G, Wójcik DK. Common atlas format and 3D brain atlas reconstructor: infrastructure for constructing 3D brain atlases. *Neuroinformatics*. 2012;10:181–197.

28. Mitzdorf U, Singer W. Prominent excitatory pathways in the cat visual cortex (A 17 and A 18): a current source density analysis of electrically evoked potentials. *Exp Brain Res*. 1978; 33:371–394.

29. Szkudlarek HJ, Orlowska P, Lewandowski MH. Light-induced responses of slow oscillatory neurons of the rat olivary pretectal nucleus. *PLoS One*. 2012;7:e33083.

30. Yamane H, de Groat W, Sculptoreanu A. Effects of ralfinamide, a Na+ channel blocker, on firing properties of nonciceptive dorsal root ganglion neurons of adult rats. *Exp Neurol*. 2007; 208:63–72.

31. Sergeeva EG, Fedorov AB, Henrich-Noack P, Sabel BA. Transcorneal alternating current stimulation induces EEG "aftereffects" only in rats with an intact visual system but not after severe optic nerve damage. *J Neurophysiol*. 2012;108:2494–2500.

32. Zaehle T, Rach S, Herrmann CS. Transcranial alternating current stimulation enhances individual alpha activity in human EEG. *PLoS One*. 2010;5:e13766.

33. Helfrich RF, Schneider TR, Rach S, Trautmann-Lengsfeld SA, Engel AK, Herrmann CS. Entrainment of brain oscillations by transcranial alternating current stimulation. *Curr Biol*. 2014; 24:333–339.

34. Thut G, Nietzel A, Brandt SA, Pascual-Leone A. Alpha-band electroencephalographic activity over occipital cortex indexes visuospatial attention bias and predicts visual target detection. *J Neurosci*. 2006;26:9494–9502.

35. van Dijk H, Schoffelen JM, Oostenveld R, Jensen O. Prestimulus oscillatory activity in the alpha band predicts visual discrimination ability. *J Neurosci*. 2008;28:1816–1823.

36. Schmidt S, Mante A, Rönnefarth M, Fleischmann R, Gall C, Brandt SA. Progressive enhancement of alpha activity and visual function in patients with optic neuropathy: a two-week repeated session alternating current stimulation study. *Brain Stimul*. 2013;6:87–93.

37. Gall C, Fedorov AB, Ernst L, Borrmann A, Sabel BA. Repetitive transorbital alternating current stimulation in optic neuropathy. *NeuroRehabilitation*. 2010;27:335–341.

38. Gall C, Brösel D, Sabel BA. Remaining visual field and preserved subjective visual functioning prevent mental distress in patients with visual field defects. *Front Hum Neurosci*. 2013;7:584.

39. Bola M, Gall C, Moewes C, Fedorov A, Hinrichs H, Sabel BA. Functional connectivity network breakdown and restoration in blindness. *Neurology*. 2014;83:542–551.

40. Butts DA, Weng C, Jin J, et al. Temporal precision in the neural code and the timescales of natural vision. *Nature*. 2007;449: 92–105.

41. Lesica NA, Jin J, Weng C, et al. Adaptation to stimulus contrast and correlations during natural visual stimulation. *Neuron*. 2007;55:479–491.

42. Wang HP, Spencer D, Fellous, JM, Sejnowski, TJ. Synchrony of thalamocortical inputs maximizes cortical reliability. *Science*. 2010;328:106–109.

43. Morimoto T, Miyoshi T, Matsuda S, Tano Y, Fujikado T, Fukuda Y. Transcorneal electrical stimulation rescues axotomized retinal ganglion cells by activating endogenous retinal IGF-1 system. *Invest Ophthalmol Vis Sci*. 2005;46:2147–2155.

44. Ni YQ, Gan DK, Xu HD, Xu GZ, Da CD. Neuroprotective effect of transcorneal electrical stimulation on light-induced photoreceptor degeneration. *Exp Neurol*. 2009;219:439–452.

45. Henrich-Noack P, Lazik S, Sergeeva E, et al. Transcorneal alternating current stimulation after severe axon damage in rats results in "long-term silent survivor" neurons. *Brain Res Bull*. 2013;95:7–14.

Investigative Ophthalmology & Visual Science